

RFID-Network Planning by Particle Swarm Optimization

E. Di Giampaolo, F. Forni, and G. Marrocco

Dipartimento di Informatica Sistemi e Produzione,
Università di Roma 'Tor Vergata' via del Politecnico, 1 00133 Roma, Italy
digiampaolo@disp.uniroma2.it, forni@disp.uniroma2.it, marrocco@disp.uniroma2.it

Abstract— The design of an ad-hoc network of readers for RFID services in large areas may require the deployment of a significant number of interrogating antennas due to the limited range of reader-tag communication. For passive tags, the factors affecting the performance of the whole link depend on many physical and geometrical parameters. The reading region is not only related to the emitted power and the radiation patterns of reader/tag antennas, but also to the propagation environment. When a number of readers are planned in a network, mutual coverage of read-zones and mutual interference are generally undesired while safety regulation constraints have to be fulfilled in the whole area. This paper introduces simple models of the most relevant electromagnetic aspects involved in the network planning problem and considers an efficient solution based on the Particle Swarm Optimization algorithm. Numerical and experimental results show the effectiveness of the method.

Index Terms—RFID, network, propagation, Particle Swarm Optimization.

I. INTRODUCTION

Radio Frequency Identification (RFID) technology is going to be used in a number of applications involving automatic detection, location, tracking and/or identification of objects and/or people [1-4]. Passive Ultra-High Frequency (UHF: 880-960MHz) RFID technology is frequently preferred to other RFID variants due to its longer read range and low cost [5]. A basic UHF passive RFID consists of a reader (i.e. a radio-scanner unit) and a number of remote transponders called tags which extract their operating power from the reader signal. Due to the limited interrogation region of readers, large-scale RFID deployments often need multiple transmitters [6-7] properly placed to

cover the entire region of interest. The planning of RFID networks, however, has to comply with the possible overlapping among interrogation regions of different antennas. This effect could be a useful redundancy in some applications (localizations) or has to be instead avoided in others (inventory) since it worsens the efficiency of the coverage and produces undesired multiple readings of a same tag.

Focusing on the latter case, the planning of RFID networks is aimed to maximize the overall read region so that tags can be read anywhere within a given environment [8], while the overlapping regions are minimized. The goal of the planning is fulfilled using the minimum number of antennas in order to reduce the cost and the complexity of the network. The locations of readers' antennas is a degree of freedom of the planning process, but also the emitted power and the orientation angle of reader antennas can be exploited.

The read region of the single reader depends on the power emitted, which is upper-bounded by the regional regulations, on the tag sensitivity over the considered objects [9] and on the orientation of the antennas [10], but it is also affected by the electromagnetic scattering from the nearby scenario [11].

The planning of RFID network moves away from the planning paradigm of other wireless networks. The down-link (reader-to-tag) is in fact subjected to the severe power threshold of the tag's microchip while the up-link (tag-to-reader), being based on backscattering, involves small power levels. Line of sight between reader antenna and tag antenna is preferred since non-line of sight communications are frequently not possible owing to the poor link-budget or because it is not useful for the particular application (as in the case of localization). The deployment of network antennas can be made almost everywhere in the environment: for instance, in indoor environments reader antennas can be placed on ceiling, floor and walls but also

some furniture structures like shelves and tables can be used to host them. Thus the structure of the network is strictly related to the topography of the environment.

Planning procedures have to include fast electromagnetic tools able to handle the propagation phenomenology with a reasonable accuracy. Although a very reliable prediction of the read region is now affordable by using the state of the art electromagnetic ray tracers [12], their extensive application to this planning problem however is revealed to be time consuming. Closed-form propagation estimation, retaining the complexity of the free-space formula, is instead preferred.

The planning method, here proposed, involves a model that simplifies the electromagnetic calculations taking into account all (or most of) the system parameters of the reader-tag-environment system including the power/exposure constraints in the UHF range. The model encodes all the electromagnetic parameters into geometrical parameters, such as distance and shape, transforming the electromagnetic problem into a geometrical problem. The interrogation region is approximated by an ellipsoid, embedding the most significant effect of the environment, and hence a number of ellipsoids have to be placed into the environment in order to achieve a uniform coverage with minimum overlapping. The so formulated RFID network planning resembles a *packing problem* in Management, Computer Science, Operations Research [13], and is here handled by the Particle Swarm Optimization (PSO) algorithm. The proposed approach, useful for both indoor and outdoor scenarios is demonstrated by some numerical examples and by experimental evaluations.

II. PLANNING PROBLEM

The aim of the planning is to guarantee the reading of a tag at points of an environment Ω using a suitable deployment of a set of reader antennas $\{R_j\}$. Since each reader's antenna has a limited interrogation region (i.e. the region where the radiated power is higher than that necessary to activate the microchip of a tag), only the union of the interrogation regions of many antennas (Fig. 1) permits to cover large environments. If Ω_j is the interrogation region of R_j antenna, the whole interrogation region is

$\Omega_I = \bigcup_{j=1}^N \Omega_j$ where N is the number of antennas in the environment. This is a constrained optimization problem where constraints concern the maximum value of EIRP (upper-bounded by regional safety regulations or by other requirements), the maximum number of possible antennas N which represent an upper limit to the cost of the network, the permitted position of the antennas, and finally the maximum field strength admitted in man-populated regions of the environment, as required by the exposure limitations.

The RFID planning problem is formulated through the definition of three sets of *control points* for the readers' position, the coverage and the safety issues. The allowed position for the readers $\{R_R\}$ depends on the specific environment and on other engineering constraints. The read test points $\{r_T\}$ are introduced to quantify the read region's size corresponding to a particular network topology and emitted power. The $\{r_T\}$ are dislocated, with a rule depending on the particular finalization of the network, with the convention that each r_T belongs to the read region provided that the field strength at that point is enough to activate the tag's microchip. Finally the *safety test points* $\{r_S\}$ are assigned to check if the radiated electric field, at places populated by persons, exceeds the threshold of the regional safety regulations.

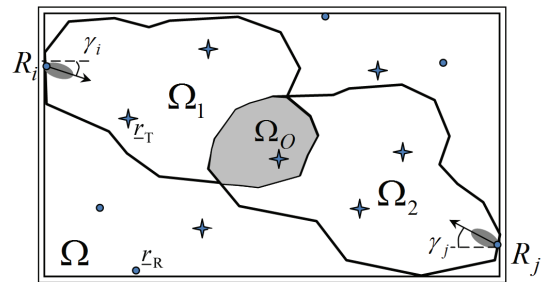


Fig. 1. Scheme of the optimization problem.

Ω region to be uniformly covered, Ω_i interrogation regions of the i th antenna R_i with tilt angle γ_i . Ω_0 is overlapping between two reading region. Dots and stars represent the allowed position of the readers and the read test point, respectively.

The extension of the interrogation region of an antenna depends on the amount of radiated power. In free-space the interrogation region is a

scaled volume of the radiation pattern of the antenna but in presence of an obstacle it is shaped by the scattering phenomena. In particular, in an indoor environment where many scattered fields contribute to the power received by the microchip, this region is not completely uniform i.e. not a path-connected space, showing jagged zones due to the interference fringes of different contributions. But jagged zones are not useful to quantify the extension of the read region because a variation of a few centimetres in the tag's position could cause an intermittent and unreliable response. Hence network evaluation has to consider a reduced path-connected subset of the interrogation region. A suitable fast electromagnetic model will be introduced in Section IV to give a simple representation of such a region by handy geometrical shapes.

The solution of the planning problem is cast as a constrained optimization aimed to maximize the following *fitness function*:

$$F = w_{COV} f_{COV} + w_{OV} f_{OV} + w_{EIRP} f_{EIRP} + w_{COST} f_{COST} + w_{SAF} f_{SAF} \quad (1)$$

where $w_{(\cdot)}$ are suitable weights ($\sum w_{(\cdot)} = 1$).

The individual contributes of F are defined as follows:

$$f_{COV} = \frac{|\{\underline{L}_R \in \Omega_I\}|}{|\{\underline{L}_R\}|} \quad (2)$$

$$f_{OV} = \frac{1}{1 + |\{\underline{L}_R \in \Omega_O\}|} \quad (3)$$

$$f_{EIRP} = \frac{1}{1 + \overline{EIRP}} \quad (4)$$

$$f_{COST} = \frac{N_{max} - N}{N_{max}} \quad (5)$$

$$f_{SAF} = \frac{1}{1 + |\{\underline{L}_S : E_T(\underline{L}_S) > E_0\}|} \quad (6)$$

where $|\{\cdot\}|$ indicates the cardinality of the included set. f_{COV} is the coverage efficiency, calculated as the number of read test points $\{\underline{L}_T\}$ included in the whole interrogation region; f_{OV} refers to the overall overlapping $\Omega_O = \bigcup_{i=1}^N (\Omega_i \cap \Omega_j)_{i \neq j}$ among all the interrogation regions; f_{EIRP} is a measure of the total power radiated by the readers' network;

$\overline{EIRP} = \frac{1}{N} \sum_{i=1}^N EIRP_i$; f_{COST} is related to the cost of

the network, e.g. it gives a measure of the readers' saving with respect to a given maximum number N_{max} ; f_{SAF} is finally an indicator of the number of safety points exposed to a total electric field E_T exceeding the limit E_0 .

III. OPTIMIZATION PROCEDURE

The result of the optimization is the position (3 parameters), orientation (2 parameters), number (1 parameter), and emitted power of each allocated reader's antenna. The dimension of the problem may be huge and hence non deterministic (evolutionary) optimization algorithms are preferred to deterministic tools. The Particle Swarm Optimization (PSO) algorithm [14-15] is here applied to maximize the fitness function in (1).

PSO is a population-based method that iteratively searches the solutions space by means of a number of candidate solutions called particles. The set of particles is called a swarm. Each particle flies through the solutions space following deterministic and stochastic rules to update its position and is rated by the fitness function. At each iteration a particle takes memory of the position where it discovered the best value of the fitness function. This value is called personal best (*pbest*) solution, while the best solution among all the particles is called the global best (*gbest*). Both *pbest* and *gbest* affect the velocity and position of each particle following the update equations

$$\begin{aligned} v_{n+1} &= wv_n + c_1 \rho_1 (x_{pbest} - x_n) + c_2 \rho_2 (x_{gbest} - x_n) \\ x_{n+1} &= x_n + v_{n+1} \end{aligned} \quad (7)$$

where n is the iteration number, x and v are the position and velocity of the particle, respectively, ρ_1 and ρ_2 are random numbers uniformly distributed in (0,1), c_1 and c_2 are weighting factors while w is an inertia weight which affects the velocity of the previous iteration.

Suitable boundary conditions are required to handle particles that reach the boundary of solutions space. Here the so called invisible walls boundary conditions [14] are used together with local-best swarm topology [15].

The PSO updates the particles by means of (6) until one of the following exit condition is reached: (i) the current solution fulfils the user-defined acceptance criterion, (ii) the number of iterations exceeds a specified value, (iii) velocity updates are close to zero.

IV. FAST EVALUATION OF THE FITNESS FUNCTION

The application of the PSO requires the fitness function in (1) to be evaluated thousands of times for each particles of the swarm and for each iteration of the search. A fast but sufficiently accurate electromagnetic model is here introduced to this purpose.

The reader can be characterized by the input power P_{in} and by the radiation vector $\underline{f}_R(\theta, \phi)$ of its antenna. The field at any point of a real environment Ω , including walls or generally scattering objects, can be obtained by application of a field projector P_Ω to the reader's pattern:

$$\underline{E}(x) = \sqrt{\frac{Z_0 P_{in} G_R(\theta, \phi)}{2\pi}} P_\Omega \circ [\underline{f}_R](\theta, \phi) \quad (8)$$

where

$\hat{\underline{f}}_R(\theta, \phi) = \underline{f}_R(\theta, \phi) / |\underline{f}_R(\theta, \phi)|$ is the normalized radiation vector and G_R is the antenna gain. In case of free-space the field projector is

$$P_\Omega \circ [\hat{\underline{f}}_R](\theta, \phi) = \frac{e^{-jk_0 r}}{r} \hat{\underline{f}}_R(\theta, \phi) \quad (9)$$

The power collected by the tag's microchip is

$$P_{R \rightarrow T} = \chi \frac{\lambda^2}{(4\pi)^2} |P_\Omega \circ \hat{\underline{f}}_R|^2 P_{in} G_R(\theta, \phi) G_T(\theta, \phi) \tau \quad (10)$$

where $G_T(\theta, \phi)$ is the tag gain and χ is the polarization mismatch between the tag antenna and the incoming field. Typically, the reader emits a circular-polarized field while the tag is a linear polarized antenna and hence $\chi=0.5$ in the free space. In a complex environment the field undergoes a depolarization, but for the sake of simplicity, the average $\chi=0.5$ value is still assumed. The application of the field projector P_Ω to the reader's pattern yields the field at tag location taking account of specific propagation phenomena that could involve reflections and diffractions from walls and generally scattering objects. The *power transmission coefficient* τ

finally accounts for the impedance mismatch between tag antenna and microchip.

The power required to the tag microchip to wake up, p_C is its sensitivity, then the tag is activated when $P_{R \rightarrow T} > p_C$.

To apply equations (10) it is necessary to specify the electromagnetic model of readers and tags as well as the field projector. Moreover the region where $|P_\Omega \circ \hat{\underline{f}}_R|^2$ is path-connected needs to be quickly estimated for any combination of the optimization parameters.

A. Tag antenna modes

Since the tag's gain is not isotropic and the power collected depends on the orientation of the tag which is in general unknown, angle-averaged gain is here considered (simply G_T in the following). A macroscopic performance indicator of the tag is the *effective sensitivity* $\tilde{p}_C = p_C / (G_T \tau)$ giving the minimum radiofrequency power that such a tag has to collect to exhibit the same averaged free-space read distance of an isolated perfectly-matched isotropic tag ($G_T \tau = 1$). This variable accounts for the performance degradation of the tag due to losses of the object and to the impedance mismatch produced by that. In other words, a real tag attached over a body will performs as a reference ideal tag having a higher power threshold.

B. Reader antenna model

The angular dependence of the reader's antenna gain has to be instead preserved then starting from the consideration that the most used reader's antenna is the circularly polarized patch [16], the main beam of the radiation pattern can be approximated by an ellipsoid whose larger axis is half the maximum gain, while the smaller axis is related to the antenna beamwidths over the principal planes. In this hypothesis it is assumed that the interrogation region be approximated by an ellipsoid

$$\frac{(x - a_x)^2}{a_x^2} + \frac{y^2}{a_y^2} + \frac{z^2}{a_z^2} = 1 \quad (11)$$

where the antenna, placed at $x=0$, radiates toward $x>0$. The ellipsoid axes are related to the RFID system parameters, such as the emitted EIRP, the tag sensitivity and the reader's antenna half-power beamwidths on the principal planes (BW_{xy} and BW_{xz}). In particular, with

reference to the geometrical construction in Fig. 2, the larger axis is

$$a_x = \frac{r_R(\theta_0, \phi_0)}{2} \quad (12)$$

being $r_R(\theta, \varphi) = \frac{\lambda}{4\pi} \sqrt{\chi P_{in} G_R(\theta, \phi) / \tilde{p}_C}$ the maximum read range in the free-space, i.e. the distance from reader's antenna where $P_{R \rightarrow T} = P_C$.

(θ_0, ϕ_0) is the maximum gain direction of the reader's antenna occurring at the broadside direction (i.e. $\phi_0 = 0^\circ, \theta_0 = 90^\circ$ in the case of the considered antenna families).

Minor axes are determined enforcing the half-power beam-width point A (Fig. 2) to belong to the ellipsoid:

$$a_{y(z)} = a_x \sqrt{\tan \frac{BW_{xy(z)}}{2} \frac{\sin \frac{BW_{xy(z)}}{2}}{\sqrt{2} - \cos \frac{BW_{xy(z)}}{2}}} \quad (13)$$

Moreover, for typical reader's antennas with circular polarization, the radiation pattern exhibits a rotational symmetry and hence $a_y = a_z$.

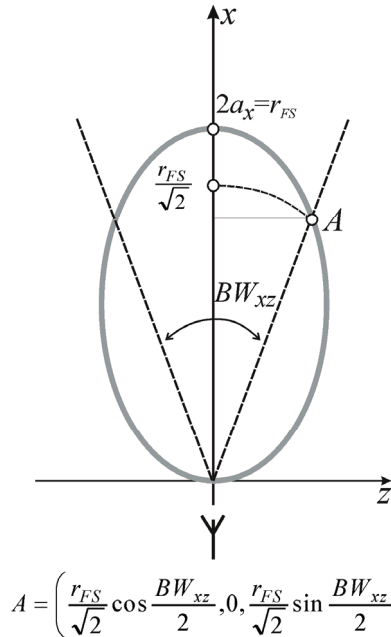


Fig. 2. Geometrical construction for the determination of the axes of the ellipsoid approximating the free-space read zone.

In a real environment the path-connected interrogation region (Ω_U) may be smaller than that in free-space owing to the interference of the radiated field with that scattered by walls and objects inside the environment. As the

interrogation range is quite short (i.e. the order of few meters) the most important interactions happen with objects placed in the neighborhood of the antenna [17]. In particular, objects placed in front of the antenna give a greater contribution to the interference in comparison with those placed laterally (floor or ceiling) owing to the directivity of the antenna. For this reason it is assumed that among all the possible contributions, only that coming from the main object in front of the antenna is dominant.

To further simplify the model, a flat obstacle is considered (as in the case of a wall) placed at distance D in front of the reader's antenna (Fig. 3). Then a simple two-ray model is able to estimate how much the useful region Ω_U is reduced. In particular, along the shortest line joining the antenna location to the object (i.e. the line perpendicular to the object surface), the *two-rays* field projector can be written as:

$$P_{\Omega} \circ [\hat{f}_{-R, \phi}] = \left(\frac{1}{r} + \frac{g}{2D-r} e^{-jk2(D-r)} \right) e^{-jkr} \quad (14)$$

where r is an abscissa along that line and g is the Fresnel's reflection coefficient of the object. When the tag moves along this line, the power collected by the tag's microchip is oscillating due to the interference of the direct and reflected ray. The distance r_{2rays} , at which the minimum power collected by the tag equals the effective microchip sensitivity, can be estimated using (9) with the field projector in (14), by solving the following equation

$$\tilde{p}_C = \chi \frac{EIRP}{(4\pi)^2} \lambda^2 \left| \frac{1}{r_{2rays}} - \frac{\Gamma}{2D-r_{2rays}} \right|^2 \quad (15)$$

where $\Gamma = |g|$ and the direction of the reader's maximum gain (θ_0, ϕ_0) is assumed perpendicular to the object surface (Fig. 3.a). Then, r_{2rays} gives the maximum distance for tag interrogation.

The function inside “[...]” in the above equation is always positive or zero for $0 < r_{2rays} < \frac{2D}{1+\Gamma}$, and hence that equation can be reduced, in this condition, to a second order polynomial

$$r_{2rays}^2 - [2D + (1+\Gamma)r_{FS}]r_{2rays} + 2Dr_{FS} = 0 \quad (16)$$

which has two solutions. One of the two solutions is not included in $(0, \frac{2D}{1+\Gamma})$ and hence it is dropped. For the particular case of perfect

conductor wall ($\Gamma=1$) the maximum read distance predicted by the two-rays model simply reduces to

$$r_{2rays} = D + r_{FS} - \sqrt{D^2 + r_{FS}^2} \quad (17)$$

Once r_{2rays} has been determined, a new ellipsoid approximating the interrogation region in real environment is obtained by setting $a_x = r_{2rays} / 2$ in equations (12).

When the reader's antenna is tilted by an angle γ (Fig. 3.b) the two-rays model can be again applied replacing D with $R = D / \cos \gamma$ because for small $\delta\gamma$ the path $r_1 + r_2 \approx 2R - r$.

In short, the ellipsoid model merges together the antenna model and the propagation model and results from a trade-off between the simplicity of the free-space approach and the accuracy of a fully (time-consuming) ray-tracer. In case of obstacles the ellipsoid extension is smaller than that of free-space model.

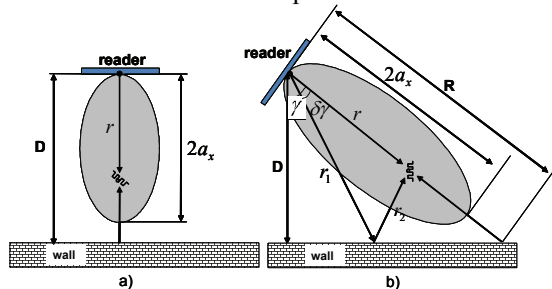


Fig. 3. Ellipsoid model of radiation pattern of readers antenna in front of a wall, a) orthogonal incidence, b) oblique incidence.

C. Experimental evaluation of the electromagnetic model

The ellipsoidal model of the read region has been experimental evaluated for a (CAEN-A948) reader whose antenna is pointing toward the ground at distance $D=2.25\text{m}$ from it. The reader's antenna has 67° beamwidth (in both the planes) and maximum gain $G_{max}=8\text{dB}$. The reader region is referred to $\tilde{p}_C = 56\mu\text{W}$ commercial meander-line tags (EPC 1 GEN2 LAB-ID UH100) replicated along a 2m -long wooden leg, with 10 cm space steps. The leg is then translated in the environment along a line with the purpose to produce a rectangular grid of measurement points. Measurement consists in recording reading and non reading tags. The reader emits 1.2 W EIRP .

A comparison between free-space model, two-ray model, full ray-tracing and measurements is shown in Fig. 4. The ray-tracing prediction is shown by the grey region wherein it is possible to observe the fringes zone owing to the interference with the ground reflected field. Continuous line ellipse concerns the two-rays model while the dotted line ellipse refers to the free-space model. Measurements are shown by means of circle and cross markers, respectively indicating responding and non-responding tags. It is noticeable the improvement of the two-ray model with respect to the free-space model.

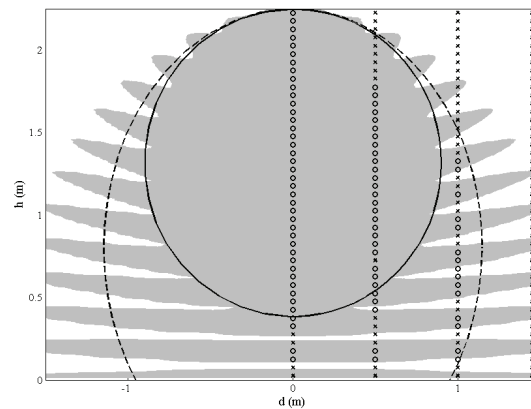


Fig. 4. Interrogation region prediction in case of the reader's antenna pointing toward the ground. Comparison between free-space model (continuous line ellipse), two-rays model (dotted line ellipse), full ray-tracing (grey region) and measurements shown by means of circle and cross markers. Circles concern reading locations, crosses non-reading locations. Reader power: 1.2 W EIRP .

V. EXAMPLES OF APPLICATION

Two optimization examples are here reported, concerning a rectangular and L-shaped room.

A. Rectangular room

The planning method has been first applied to a simple scenario shown in Fig. 5 consisting of a small hall at the entrance of a building with four doors. Reader's antennas are desired to be placed so that a uniform interrogation region is achieved on the vertical cross-section of the hall (Fig. 5.B). Antennas can be placed on side walls and ceiling and they are required to radiate the minimum possible power. The allowed reader position $\{L_R\}$ are uniformly deployed on the

ceiling and walls starting at $1m$ from the floor, with a step of $0.3m$. $\{L_T\}$ are spread on the cross-section area with a uniform $0.6 \times 0.3m^2$ grid. Safety test points $\{L_S\}$ are not been taken into consideration being this a place where people pass through. The magnitude of the reflection coefficient of both walls and ceiling has been set to $\Gamma = 0.5$. Reader's and tag's features are the same of the previous section. The allowed maximum number of antennas is four, while the allowed maximum value of EIRP is $3.2W$.

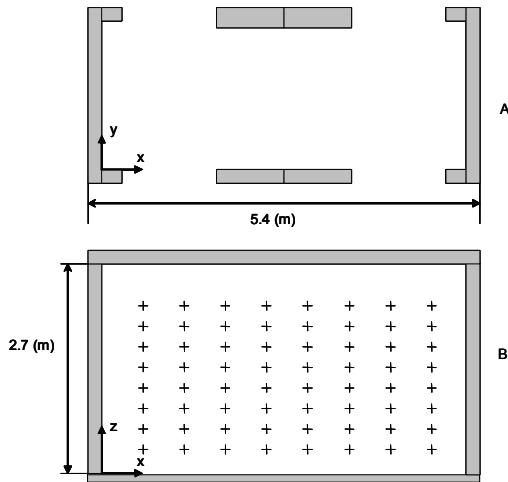


Fig. 5. Horizontal (A) and vertical (B) section of the hall used for experiment. Crosses indicate the read test points $\{L_T\}$.

The optimization parameters in (6) and in (7) are: $c_1=c_2=1.49$, $w=0.726$, $v_{max}=3.2$; $w_{COV}=0.6$, $w_{OV}=0.15$, $w_{EIRP}=0.05$, $w_{COST}=0.2$, $w_{SAF}=0.0$.

The Particle Swarm optimization results are summarized in Table 2 while the resulting ellipses of uniform reading zones are shown in Fig. 6 where it can be appreciated that only two antennas are enough to cover the 92% of the $\{L_T\}$.

The obtained planning result has been put into practice and measurements have been performed to test the reliability of the optimization. The measurement grid consist of $19 \times 25 = 475$ points laying on the vertical $y=1.5m$ plane at steps of $0.3m$ along the x axis and $0.1m$ along the z axis.

Results are shown in Fig. 7 by means of dot and cross markers which refer to reading and non reading points, respectively. The ellipses of the planned uniform reading zones are also shown and it is possible to observe a good agreement with the measurement results. The

76.21% of the measurement points are reading points.

Table 1: Optimized parameters of the two-reader network.

Reader	Position (x,y,z) [m]	EIRP [W]	Tilt [deg]	BW [deg]
R_1	(0, 1.5, 1.0)	2.95	+30	67
R_2	(5.4, 1.5, 1.5)	1.8	-30	67

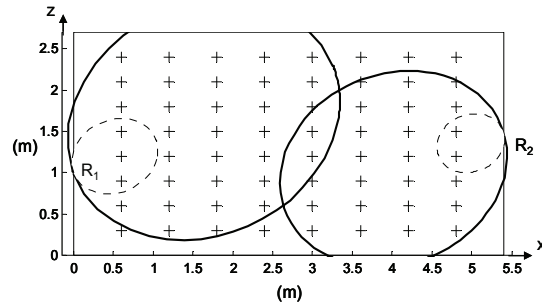


Fig. 6. Planning result on the vertical section (B) of Fig. 5. Crosses represent $\{L_T\}$ (read test points). R_1 and R_2 reader's antenna locations. Continuous line ellipses show the uniform covered zone of readers. Dotted line ellipses show the zone where the field exceeds the regional safety regulations.

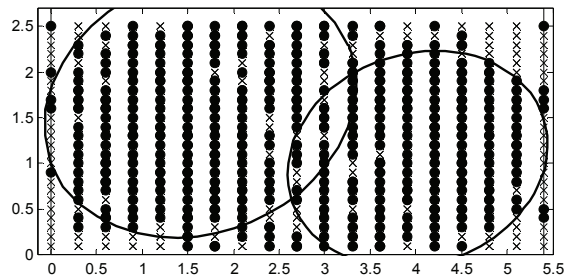


Fig. 7. Comparison between planning results and measurements. Ellipses show the planned uniform read zone as estimated by the electromagnetic two-rays tool. Crosses and dots show measured non reading and reading points, respectively.

B. L-shaped room

To highlight the ability of the optimization algorithm to reduce the cost and to enhance the coverage of the network, a more complicated topology has been considered. The scenario consists of an L-shaped environment (Fig. 8.a), wherein reader's antennas are constrained to be placed only on two side walls ($x=0m$ and $y=5m$).

Three different optimizations are presented, having gradually released the constraints on the reader's geometrical and electrical parameters. To value the benefit of the optimizations in the considered cases, the fitness function is used as an overall indicator.

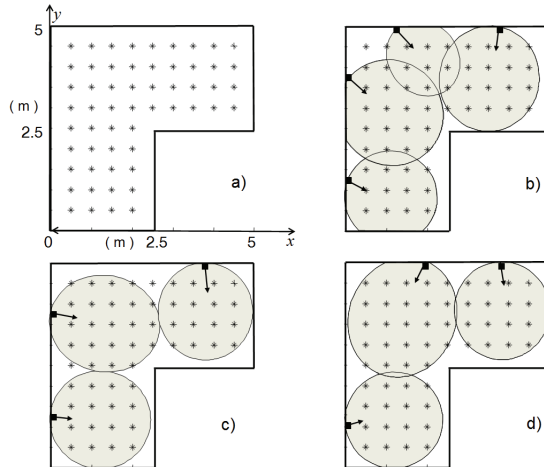


Fig. 8. L-shaped environment wherein network coverage is planned with different constraints. a) set-up with $\{L_T\}$ shown by stars; b) EIRP and antennas orientation (indicated by arrows) optimized; c) number of readers, EIRP and orientation optimized; d) complete optimization. Arrows show antennas' orientation, ellipses interrogation region.

Table 2: Result of optimization planning of the environments in Fig. 8.

	f_{COV}	f_{OV}	f_{EIRP}	f_{COST}	F
b)	0.98	0.43	0.32	0	0.67
c)	0.95	1	0.30	0.25	0.78
d)	1	0.92	0.30	0.25	0.80

At first, number and position of antennas are fixed while orientation and $EIRP \leq 3.2W$ are optimized. Starting from four antennas, the optimization process tries to reduce the overlapping regions lowering the radiated power and orienting the antennas (Fig. 8.b). Some overlapping regions are still visible however. Removing the constraint on the number of antennas, only three antennas are needed to cover the 95% of the test points (Fig. 8.c): the overall indicator is increased with respect to the previous case (Table 2) as the efficiency is enhanced and the cost and overlapping are reduced. Finally all the parameters are free to be optimized and the planning result is shown in

Fig. 8.d. The whole coverage is obtained and the overall indicator is greater than the previous cases.

VI. CONCLUSIONS

The planning of the deployment of readers in large and complex environments is a trade-off between the maximum interrogation zone, required for the particular application, and the electromagnetic and topography constraints. Simple and fast electromagnetic models have been applied in the frame of a PSO algorithm for planning in real environment.

The given numerical and experimental examples have demonstrated the effectiveness of the method and have shown that the coverage quality may be greatly improved when all the geometrical and electric options are fully exploited.

The application of the planning method to large and complex environments is expected to be computational hard because of the large number of readers, necessary to the coverage.

However, a reduction of the computational burden can be achieved by partitioning the whole optimization problem into a number of smaller sub-problems, taking advantage on the natural localization of the UHF RFID link. The environment can be subdivided into a number of subsets exploiting geometrical symmetries and the natural partition induced by walls and big objects. Fictitious reflecting surfaces, not hosting readers, may be introduced to split open space regions. The optimization process can be then applied in parallel to each subset preserving a computational complexity comparable with that of the previous examples.

ACKNOWLEDGMENT

The authors wish to thank LAB-ID to have provided UHF tags.

REFERENCES

- [1] K. Finkenzeller, *RFID Handbook*, Wiley & Son, 2000.
- [2] R. Want, "An Introduction to RFID Technology," *IEEE Pervasive Computing*, Vol.5, No.1, pp. 25-33, Jan.-March 2006.
- [3] L. M. Ni, Y. Liu, Y. C. Lau, and A. Patil, "LANDMARC: Indoor Location Sensing Using Active RFID," in *Proceeding of the first IEEE International Conference in Pervasive Computing*, 2003.

- [4] R. S. Sangwan, R. G. Qiu, and D. Jessen "Using RFID tags for tracking patients, charts and medical equipment within an integrated health delivery network", *IEEE Int. Conf. Networking Sensing and Control* 2005, pp.1070-1074, 2005.
- [5] G. Marrocco, "The art of UHF RFID antenna design: impedance-matching and size-reduction techniques", *Antennas and Propagation Magazine, IEEE*, Vol. 20, No.1, pp. 66-79, Feb. 2008.
- [6] W. James, E. Daniel, and S. Sanjay, "Colorwave: A mac for rfid reader networks", *Proc. of IEEE WCNC*, Vol. 3, pp. 1701-1704, 2003.
- [7] Z. Zhou, H. Gupta, S. R. Das, and X. Zhu, "Slotted Scheduled Tag Access in Multi-Reader RFID Systems," in *Proceeding of the fifteenth IEEE International Conference on Network Protocols (ICNP)*, 2007.
- [8] Q. Guan, Y. Liu, Y. Yang, and W. Yu, "Genetic Approach for Network Planning in the RFID Systems", *Proceedings of the Sixth International Conference on Intelligent Systems Design and Applications (ISDA'06)*, IEEE, 2006.
- [9] R. Clarke, D. Twede, J. Tazelaar, and K. Boyer, "Radio frequency identification (RFID) performance: the effect of tag orientation and package contents", *Packaging Technology and Science*, Vol. 19, No. 1, pp. 45-54, 2006.
- [10] K.V.S. Rao, D.W. Duan, and H. Heinrich, "On the read zone analysis of radio frequency identification systems with transponders oriented in arbitrary directions", *1999 IEEE Microwave Asia Pacific Conference*, Vol. 3, pp. 758-761, 1999.
- [11] R. Banerjee, R. Jesme, and R. A. Sainati, "Performance analysis of short range UHF propagation as applicable to passive RFID", *IEEE RFID Conference*, pp. 30-36, 2007.
- [12] E. Di Giampaolo and F. Bardati, "A Projective Approach to Electromagnetic Propagation in Complex Environments", *Progress In Electromagnetics Research B*, Vol. 13, pp. 357-383, 2009.
- [13] A. Donev, et al., "Improving the Density of Jammed Disordered Packings Using Ellipsoids", *Science*, Vol. 303, pp. 990-993, 2004.
- [14] J. Robinson and Y. Rahmat-Samii, "Particle Swarm Optimization in Electromagnetics", *IEEE Trans. Ant. Prop.*, Vol. 52, No. 2, 2004 .
- [15] J. Kennedy and R. Mendes, "Population Structure and Particle Swarm Performance", *Proceedings of the Evolutionary Computation 2002 Congress CEC '02*, Vol. 2, 2002.
- [16] J. M. Lee, N. S. Kim, C. S. Pyo, "A Circular Polarized Metallic Patch Antenna for RFID Reader", *Asia-Pacific Conference on Communications*, pp. 116-118, October 2005.
- [17] L. W. Mayer, M. Wrulich, and S Caban, "Measurements and channel modeling for short range indoor UHF applications", *Proceedings of The European Conference on Antennas and Propagation, (EuCAP 2006)*, November, 2006.

Emidio Di Giampaolo



received the Laurea in Electronic Engineering in 1994 and a Ph.D. in Applied Electromagnetics in 1998 both from University of L'Aquila (Italy). Since 1998 to 2004 he has been a post doctoral researcher at the

University of L'Aquila where he also taught Radio-wave propagation as a substitute. Since 2005 he has been a researcher at the University of Rome "Tor Vergata" where he teaches Industrial Microwave Applications and a laboratory class on antennas. In the spring of 2000 he was a Visiting Researcher at the European Space Research and Technology Centre (ESTEC), Noordwijk (NL).

His research interests mainly concern numerical methods for modelling radio-wave propagation in complex environments, antennas and indoor radio localization.



Fausto Forni of Siracusa (Italy) received the Laurea degree in Telecommunications Engineering from the University of Rome "Tor Vergata", Italy, in 2009. His interests include antennas, RFID systems

and evolutionary algorithms.



Gaetano Marrocco of Teramo (Italy) received the Laurea in Electronic Engineering in 1994 and a Ph.D. in Applied Electromagnetics in 1998, both from University of L'Aquila. He has been a researcher at the University of Rome "Tor Vergata" since 1997 where he currently teaches Antenna Design and Bioelectromagnetics. In the summer 1994 he was at the University of Illinois at Urbana Champaign as a post-graduate student. In the autumn 1999 he was a visiting scientist at the Imperial College in London. His research is mainly directed to the modelling and design of broad band and ultra wideband antennas and arrays as well as of miniaturized antennas for RFID applications. He has been involved in several space, avionic, naval and vehicular programs of the European Space Agency, NATO, Italian Space Agency, and the Italian Navy. He holds two patents on broadband naval antennas and one patent on sensor RFID systems. He currently serves as Associate Editor of the IEEE Antennas and Wireless Propagation Letters.